International Journal of Food Studies | IJFS April 2019 | Volume 8 | pages 111–126

Moisture Sorption Isotherm and Thermodynamic Properties of Jamun (*Syzygium cumini* L.) Powder made from Jamun Pulp and Seed

Indira Dey Paul[a] and Madhusweta Das[a*]

[a] Agricultural and Food Engineering Department, Indian Institute of Technology Kharagpur, Pincode-721302, West Bengal, India
[*]Corresponding author
madhu@agfe.iitkgp.ac.in
Tel: +91 8777359497
Fax: +91 3222 282244; 255303

Received: 10 July 2018; Published online: 18 April 2019

Abstract

The present work aimed to: i) find the suitable proportion, based on sensory evaluation, of microwave-convective hot air dried jamun (*Syzygium cumini* L.) pulp and seed kernel powder to be mixed for the preparation of jamun powder (JP); ii) generate and model the moisture sorption isotherm (MSI) of JP; and iii) estimate net isosteric heat of sorption (q_{st}), spreading pressure (Φ), net integral enthalpy (Q_{in}), and net integral entropy (S_{in}). To formulate JP, the proportion (w/w, db) comprising 2% kernel and 98% pulp powder was the most desirable. The Peleg model was the best fit to MSI of JP. The q_{st} decreased following linear relationship from 11.02 kJ. mol^{-1} at 5% equilibrium moisture content (EMC) to 0.27 kJ. mol^{-1} at 30% EMC. The Φ increased with increase in water activity and decreased with increase in temperature from 25 ^{o}C to 35 ^{o}C, and the values of Φ at 45 ^{o}C were even higher than at 25 ^{o}C. Net integral enthalpy (Q_{in}) initially decreased till 6% moisture content in JP and displayed an increasing trend with further increase in moisture content. On the contrary, S_{in} kept on decreasing continually with increasing moisture content. The moisture zone of 7-11% was considered safe for storage of JP within the temperature range of 45-25 ^{o}C.

Keywords: Jamun powder; Moisture sorption isotherm; Net isosteric heat of sorption; Spreading pressure; Net integral enthalpy; Net integral entropy

1 Introduction

Jamun (*Syzygium cumini* L.), a type of berry with an attractive sweet-sour taste and purple colour, is a fruit native to India and East Indies, but is also found in other countries like Thailand, Philippines and Madagascar. All the fractions of whole jamun fruit, besides their nutritional constituents, contain a lot of phytochemicals and, hence, are widely popular for their medicinal values. Sehwag and Das (2015) reported a broad classification of the phytochemicals such as anthocyanins, phenolic acids, flavonols, flavanonols, carotenoids and terpenes in the pulp and skin, and alkaloids, flavonoids, glycosides, phytosterols, saponins, tannins and triterpenoids in the seed. Recent studies on jamun pulp and skin have established many therapeutic properties such as antidiabetic, antioxidant, hepatoprotective, antibacterial and anticancerous. Jamun seed kernel is richer in medicinal properties than pulp and skin, and possesses a range of pharmacological actions (Sehwag & Das, 2015, 2016). However, due to its short seasonal availability

 10.7455/ijfs/8.1.2019.a10

Nomenclature

a_m	Surface area of a water molecule (m^2)
a_w	Water activity
Φ	Spreading pressure (J. m^{-2})
a_w^*	Geometric mean water activity at constant Φ
EMC	Equilibrium moisture content (%, db)
GMS	Glycerol monostearate
JP	Jamun powder
K_β	Boltzmann constant (J. K^{-1})
LDPE	Low density polyethylene
LSD	Least significant difference
M	EMC (%, db) of the sample
MCD	Microwave-convective hot air drying
MD	Maltodextrin
MRE	Mean residual error (%)
MSI	Moisture sorption isotherm
Q_{in}	Net integral enthalpy (kJ. mol^{-1})
q_{st}	Net isosteric heat of sorption (kJ. mol^{-1})
R	Universal gas constant (kJ. mol^{-1}. K^{-1})
r^2	Co-efficient of determination
RH	Relative humidity (%)
RMSE	Root mean square error
S_{in}	Net integral entropy (kJ. mol^{-1}. K^{-1})
SD	Standard deviation
T	Absolute temperature (K)
TCP	Tricalcium phosphate
Z	Integration constant

and highly perishable nature, jamun remains underutilized.

Removal of moisture by quick and efficient drying is the most promising way for seasonal and perishable fruits to be made available throughout the year. Dehydrated fruit in powder form can be incorporated within a variety of recipes, like desserts, biscuits and spreads, to add case specific flavor and functionalities without the moisture and volume of fresh fruit. Among different methods, a hybrid technique, microwave-convective hot air drying (MCD) has been used effectively for drying various food materials such as apricot halves (Horuz, Bozkurt, Karatas, & Maskan, 2017), button mushrooms (Das & Arora, 2018), oyster mushrooms (Bhattacharya, Srivastav, & Mishra, 2015), okra (Kumar, Prasad, & Murthy, 2014) and garlic cloves (Sharma & Prasad, 2001). Prolonged exposure in conventional hot air drying leads to undesirable changes in product quality. Combining microwave with convective hot air can significantly reduce the drying time and improve product quality (Schiffmann, 1992). Although jamun seed powder (no mention of the presence or absence of seed coat) is available as an ayurvedic medicine for control of diabetic mellitus, technical information on drying of jamun seed and pulp is scanty in the literature. Recently Dey Paul and Das (2017) produced free flowing jamun pulp (along with skin) powder containing maltodextrin (MD, 12.2%), tricalcium phosphate (TCP, 0.4%) and glycerol monostearate (GMS, 1.4%) on a dry basis (db) of pulp-skin, using MCD at 70 ^{o}C, 1 watt. g^{-1} (W. g^{-1}, power density), 0.5 m. s^{-1} air velocity, to maximally maintain its antioxidant activity. Monica, Dey Paul, and Das (2016) also observed that MCD (60 ^{o}C, 2 W. g^{-1}, 0.5 m. s^{-1}) of jamun seed retained maximum antioxidant activity of its kernel. Thus, if pulp powder is mixed with seed kernel powder (bitter in taste probably due to the presence of saponins and tannins) (Kamal, 2014; Kapoor & Iqbal, 2013) in a sensorially acceptable ratio,

the mixture could be used as jamun powder (JP) for food purpose, with more health benefits than that of pulp powder alone.

Moisture sorption tendency, which depends on relative humidity (RH) and temperature, is a major criterion in maintaining quality of fruit powders during handling and storage. Moisture sorption isotherm (MSI) provides the relationship between equilibrium moisture content (EMC) and its water activity (a_w) when the food equilibrates in air with different RHs at a certain temperature. On equilibration, the a_w of food (relates to stability) equals the RH of environment (Al-Muhtaseb, McMinn, & Magee, 2002). Moisture sorption isotherm (MSI) is an essential tool in design of drying, packaging and storage of food. Mathematical modelling enables generation of MSI at any unknown temperature within the temperature range for which the MSIs have already been developed empirically. de Santana et al. (2015) reported MSIs of freeze dried jamun pulp (without skin) containing no additives. Biswal, Mohapatra, Panda, and Dash (2017) modelled the desorption isotherm of fresh jamun fruits. Ferrari, Marconi Germer, Alvim, Vissotto, and de Aguirre (2012) modelled the MSI of spray dried blackberry (*Rubus* species) powder containing maltodextrin and gum arabic. Information on the MSI of powder containing pulp, skin and kernel of jamun, together with any drying aid (to make the powder form) is not available.

Moisture sorption isotherms at different temperatures are used to evaluate thermodynamic parameters like net isosteric heat of sorption (q_{st}), spreading pressure (Φ), net integral enthalpy (Q_{in}) and net integral entropy (S_{in}) (Al-Muhtaseb, McMinn, & Magee, 2004). The q_{st} (total heat of sorption for binding water vapor on sorbent less than the heat of vaporization of pure water, at the system moisture content) determines moisture-sorbent binding strength, and is required in designing equipment for dehydration processes as well as prediction of a_w when the food is stored at fluctuating temperature (Chowdhury & Das, 2010). Spreading pressure (Φ), the difference in surface tension between bare sorption sites of the sorbent and sites with adsorbed molecules, indicates the free surface energy of adsorption (Al-Muhtaseb et al., 2004). Net integral enthalpy (Q_{in}) at constant Φ, a measure of the strength of moisture-solid binding, is used to determine S_{in} (McMinn & Magee, 2003). Net integral entropy (S_{in}) explains the degree of disorder and randomness of the adsorbed water molecules (Arslan & Togrul, 2005; Igathinathane, Womac, Sokhansanj, & Pordesimo, 2007), and helps to determine the moisture at which the sorbent is stable.

Based on the above knowledge, the objectives of the present work were to: i) find the suitable proportion of pulp (with skin) and kernel powder to be mixed for preparation of JP; ii) generate and model the MSI of JP; and iii) estimate the thermodynamic parameters, including net isosteric heat of sorption (q_{st}), spreading pressure (Φ), net integral enthalpy (Q_{in}) and net integral entropy (S_{in}) for the JP.

2 Materials and Methods

2.1 Material

Fully matured jamun fruit (raw material), apparently free from any damage, was procured from the local market of IIT Kharagpur, India. About 75% of the fruit was comprised of pulp with adherent skin (hereunder called pulp), with the remaining 25% being the seed. The moisture, protein, fat, ash, crude fiber and carbohydrate content of pulp were analysed and found to be 83.04±0.10% (wet basis, wb), 8.59±0.07, 3.23±0.39, 4±0.001, 2.49±0.00 and 81.71±0.45% (dry basis, db) respectively. For seed kernel, the respective values were 15.12±0.04% (wb), 5.90±0.14, 1.01±0.01, 2.34±0.02, 2.33±0.37 and 88.41±0.53% (db) (Sehwag & Das, 2016). MD (dextrose equivalent < 20) and TCP, both from HiMedia Laboratories Pvt. Ltd., Mumbai, India, and GMS from Alfa Aesar, Massachusetts, USA, were used as additives for production of pulp powder. Analytical grade lithium chloride (LiCl), potassium acetate (CH_3COOK), magnesium chloride ($MgCl_2$), potassium carbonate (K_2CO_3), magnesium nitrate $Mg(NO_3)_2$, sodium nitrate ($NaNO_3$), sodium chloride (NaCl) and potassium chloride (KCl) were used to adjust RH (described below). All the chemicals were used as received. Glass distilled water was used for

preparation of salt solutions.

2.2 Preparation of raw materials

The fruits were washed with potable water and air dried at room temperature. The pulp was separated from the seed with a knife, and stored in low density polyethylene (LDPE) pouches (about 250 g pouch^{-1}; pouch film thickness $\sim$ 0.05 mm) at -30 ^{o}C. The seeds were washed with water to remove any adhering pulp, and similarly packed and stored.

2.3 Preparation of jamun pulp and seed kernel powder

The frozen pulp was put in an empty glass beaker, which was then thawed in a water bath at room temperature (28 ^{o}C). The thawed mass was then ground into paste (at same temperature) using domestic grinder (Sumeet Research and Holdings Limited, Chennai, India). The paste was mixed with 12.2% MD, 0.4% TCP and 1.4% GMS on dry basis (db) of the pulp. The mixed paste was dried using a fully controlled miniature conveyer type industrial microwave-convective hot air dryer (Enerzi Microwave Systems Pvt. Ltd., Bangalore, Karnataka, India) having 20-100 kg. h^{-1} drying capacity, 2450 MHz frequency and 250-3000 W power. An in-built heater of 6 kW provided hot air (25 ^{o}C to 200 ^{o}C) circulation. The drying chamber, 2 m x 300 mm x 200 mm, was made of 2 mm thick stainless steel. Drying was carried out at 70 ^{o}C, 1 W. g^{-1} and 0.5 m. s^{-1} air velocity. The composition of the mixture and drying method and conditions were described earlier (Dey Paul & Das, 2017; Paul & Das, 2018). The dried pulp obtained in flake form was ground into fine powder (212 μm passing).

The frozen jamun seeds were thawed, dried using the same dryer but at 60 ^{o}C, 2 W. g^{-1} and 0.5 m. s^{-1} air velocity, and the seed coat was manually removed (Monica et al., 2016). The dried kernels were ground into fine powder (212 μm passing).

To judge the functionality, in separate work (not included here), total phenolic content (TPC) in mg gallic acid equivalent (GAE)/g, DPPH antioxidant activity (AA) in mg butylated hydroxyanisole (BHA)/g, db, both in 50% aqueous ethanolic extract, and monomeric anthocyanin content (MAC) in mg malvidin3glucoside (M3G)/ g, db were measured for different portions (triplicate) of the powder before and after mixing. The pulp powder contained 26.19±0.45 TPC, 23.79±0.35 AA and 9.96±0.16 MAC, whereas for kernel powder the values were 53.95±0.26 TPC and 57.97±0.31 AA.

2.4 Mixing of jamun pulp and seed kernel powder

Pulp powder and kernel powder, in different proportions, were mixed by tumbling (10 min), followed by wire whipping (10 min) using a hand blender (Anjali Marketing & Research Centre, Mumbai, India). Based on a nine-point hedonic rating of appearance, aroma, taste, mouthfeel and overall acceptability of the mixtures by 27 semi-trained panellists, a suitable proportion was selected (Ranganna, 1986). The selected mixture, referred to as JP, was double packaged in LDPE pouches, and stored at -30 ^{o}C for further studies.

2.5 Determination and modelling of EMC

The isopiestic vapour transfer technique was used to determine EMC (Chowdhury & Das, 2010). Around one gram of JP was placed in a weighing bottle (in triplicate) and the bottles placed in eight vacuum desiccators, each containing a saturated solution of a salt (section 3.2) to maintain RH (10-90%). The desiccators were placed in an incubator at 25 ^{o}C. After equilibration (about five days based on preliminary experiments), the mass of the bottles plus samples were noted. These were then dried overnight at 105±1 ^{o}C to determine the dry mass of JP. The EMC (%, db) was calculated using Eq. (1).

$$EMC(\%) = \frac{W_{eq} - W_{dry}}{W_{dry}} \times 100 \qquad (1)$$

where W_{eq} and W_{dry} are the masses of equilibrated and dried powder.

The experiment was similarly carried out at 35

^{o}C and 45 ^{o}C.

Five MSI models (Table 1) were used to fit the experimental EMCs using non-linear regression analysis (Microsoft Excel 2013). In the models, M represents EMC (%, db) of the sample, and a_w is its water activity. A, B and C are the model specific coefficients. In the GAB model, A, B and C, respectively, represent the monolayer moisture content, heat of the first layer sorption and heat of the multilayer sorption.

Model fitting parameters, including co-efficient of determination (r^2), root mean square error (RMSE) (Eq. 2), mean residual error (MRE %) (Eq. 3) and residual plot (a plot of (M_i - M_{pi}) versus M_i for respective a_ws) were evaluated. The r^2 was evaluated through regression analysis.

$$RMSE = \left[\frac{1}{n} \times \sum_{i=1}^{n} (M_i - M_{pi})^2\right]^{1/2} \quad (2)$$

$$MRE(\%) = \frac{100}{n} \sum_{i=1}^{n} \left|\frac{M_i - M_{pi}}{M_i}\right| \quad (3)$$

where M_i and M_{pi} are the experimental and predicted values of EMC and n is the number of experimental runs.

To be a good fit, the model should have a r^2 close to 1, RMSE close to 0, MRE below 10% and randomness in the residual plot where the data points are distributed in a horizontal band around zero (Lomauro, Bakshi, & Chen, 1985).

2.6 Net isosteric heat of sorption (q_{st})

The q_{st} (kJ. mol^{-1}) was estimated using the Clausius-Clapeyron equation (Eq. 4).

$$ln\ a_w = -\frac{q_{st}}{RT} + Z \quad (4)$$

where R is the universal gas constant (8.314×10^{-3} kJ. mol^{-1}. K^{-1}), T is the absolute temperature in Kelvin (K) and Z is the integration constant.

Using the best fit model, a_w values were evaluated, at any particular moisture content, for different temperatures. The slope of the plot of ln a_w versus 1/T gave the q_{st} at that moisture content. This was repeated for different moisture contents to evaluate the effect of moisture content on q_{st}. The absolute value of q_{st} was considered, as the sign of q_{st} doesn't bear any physical interpretation (Chowdhury & Das, 2010).

2.7 Spreading pressure (Φ)

According to Igathinathane et al. (2007), spreading pressure, Φ (J. m^{-2}), was calculated using Eq. (5) as shown below.

$$\Phi = \frac{K_\beta T}{A_m} \int_0^{a_w} \frac{M}{A a_w} da_w \quad (5)$$

where K_β is the Boltzmann constant (1.380×10^{-23} J. K^{-1}), A_m is the surface area of a water molecule (1.06×10^{-19} m^2), M is the EMC and A is the monolayer moisture content.

Since the integral cannot be evaluated at a_w = 0.0, the lower limit in Eq. (5) was considered as 0.05. After substituting the GAB equation (Table 1) in Eq. (5) and integrating, spreading pressure for the range of a_w from 0.05 to a_w was calculated using Eq. (6) (Lago, Liendo-Cardenas, & Zapata Norena, 2013).

$$\Phi = \frac{K_\beta T}{A_m} ln \left[\frac{1 + BCa_w - Ca_w}{1 - Ca_w}\right]_{0.05}^{a_w} \quad (6)$$

The integral covering the a_w range from 0.00 to 0.05 was evaluated (Eq. 7) assuming a linear relationship (Henry's law) between M/A and a_w (Fasina, Ajibola, & Tyler, 1999; Igathinathane et al., 2007).

$$\Phi = \frac{K_\beta T M}{A_m A} \quad (7)$$

Totalling the values of Eq. (6) and Eq. (7), the Φ corresponding to any temperature and a_w combination was produced. Spreading pressure versus a_w was plotted for different temperatures.

2.8 Net integral enthalpy (Q_{in})

Net integral enthalpy (Q_{in}, kJ. mol^{-1}) was evaluated (Eq. 8) in a comparable methodology to that of the q_{st} but at constant Φ instead of constant moisture content:

$$\left|\frac{d[lna_w]}{d[1/T]}\right|_\Phi \approx -\frac{Q_{in}}{R} \quad (8)$$

Table 1: Sorption models used for fitting experimental EMC data of JP

Model	Equation	Reference
Peleg	$M = A(a_w)^B + C(a_w)^D$	Chowdhury and Das (2010)
Guggenheim-Anderson-de-Boer (GAB)	$M = ABCa_w/[(1\text{-}Ca_w)(1\text{-}Ca_w + BCa_w)]$	Ibanoglu, Kaya, and Kaya (1999)
Oswin	$M = A\,[a_w/(1\text{-}a_w)^B]$	de Santana et al. (2015)
Henderson	$M = [-\ln(1\text{-}a_w)/A]^{1/B}$	de Santana et al. (2015)
Halsey	$M = [-A/\ln(a_w)]^{1/B}$	Chowdhury and Das (2010)

From the plot of Φ versus a_w at various temperatures, a_w values at any particular Φ were obtained through interpolation (Igathinathane et al., 2007). The slope of the plot of ln a_w versus 1/T at constant Φ produced the Q_{in}. Next, moisture contents at the interpolated a_w values were calculated using the best fit MSI equation. Thus, at three temperatures, there were three moisture contents for each Φ, and the geometric mean moisture content was derived. Q_{in} versus geometric mean moisture content was then plotted.

2.9 Net integral entropy (S_{in})

Net integral entropy (S_{in}, kJ. mol^{-1}. K^{-1}) was calculated using the following equation (Eq. 9) (Igathinathane et al., 2007).

$$S_{in} = \frac{-Q_{in}}{T} - Rln(a_W^*) \tag{9}$$

where a_w^* is the geometric mean water activity at constant Φ. The temperature term T of Eq. (9) was interpolated linearly for a_w^* from the T versus a_w data for a given Φ. S_{in} was then plotted against moisture content.

2.10 Statistical analyses

The arithmetic mean of the replicated values of different observations and the respective standard deviation (SD) were evaluated. Geometric means, in calculations of thermodynamic parameters, were also evaluated. The mean values were used in analysis of variance (F test, one way) relating to parametric variation (treatment effect) followed by evaluation of least significant difference (LSD at $P<0.05$, in cases of positive F test), paired t-test ($P<0.05$), and model fitting.

3 Results and discussion

3.1 Mixing of pulp and kernel powder

In JP, the sensory quality of pulp is most desirable, as the kernel powder possesses bitter taste. The results of sensory evaluation on mixing of pulp and kernel powder are shown in Table 2. It is seen that aroma, taste and overall acceptability of the pulp powder were negatively affected (F test positive) by addition of kernel powder, whereas appearance and mouthfeel remained unaffected. The corresponding LSD value (included in the same table) indicates that deterioration of the pulp powder starts at 6% addition of kernel powder for aroma and 4% addition of kernel powder for both taste and overall acceptability. At 2% addition, none of these qualities were affected. Therefore, 2% kernel addition was finally selected for the production of JP. The produced powder (JP) is shown in Figure 1, which contained TPC, AA and MAC values of 27.25±0.19 (mg GAE/g, db), 25.04±0.07 (mg BHA/g, db) and 9.77±0.22 (mg M3G/g, db) respectively. These values are statistically different (t-test) from those of pulp powder. Thus, addition of 2% kernel powder led to an increase in TPC and AA values of the pulp powder by 4-5%, while the MAC value was less ($\sim$ 2%). Furthermore, the standard deviation of these functionalities was within 0.2-2%. Since low standard deviation is an indication of powder mixing, the JP can be considered to have good overall uniformity.

Table 2: Sensory evaluation of the mixed powder containing different proportions of pulp and kernel powder

Mixed powder constituents (%, w/w, db)		Mean±SD				
Pulp powder	**Kernel powder**	**AppearanceΨ**	**Aroma**	**Taste**	**MouthfeelΨ**	**Overall acceptability**
100	0	7.56±0.70	7.63±0.97$^{\#}$	7.43±0.72$^{\#}$	6.63±1.42	7.67±0.64$^{\#}$
98	2	7.56±0.70	7.74±0.82$^{\#*}$	7.46±0.80$^{\#}$	6.80±0.94	7.56±0.66$^{\#}$
96	4	7.52±0.80	7.26±1.32$^{\#*}$	6.39±0.75*	6.52±1.53	6.50±0.71
94	6	7.20±1.11	6.91±1.58$^{*\$}$	6.00±0.77*	6.52±1.42	5.82±0.84
92	8	7.13±0.89	6.83±1.39$^{\$!}$	5.56±0.74	6.22±1.31	5.39±0.83
90	10	7.04±1.29	6.74±1.68$^{\$!}$	4.93±0.84	6.06±1.30	4.74±0.90
LSD		**-**	**0.71**	**0.41**	**-**	**0.41**

Ψ, P >0.05 in F-test; #,*,$,!, The same superscript indicates no significant difference between the mean values.

Figure 1: Jamun powder (JP) having particle size below 212 μm

3.2 Equilibrium moisture content (EMC) of JP

The mean EMCs±SD of JP for varying RH (with different salts) at 25 ^{o}C, 35 ^{o}C and 45 ^{o}C are presented in Table 3. One-way ANOVA, at any temperature, resulted in a positive F-test (p <0.05) indicating that EMC is significantly dependent on the RH of the environment (a_w of the sample). LSD values further confirm that at all three temperatures, EMC increased with increase in RH/a_w, except for the range of a_w from 0.113 to 0.215 at 35 ^{o}C. Thus, the sorption characteristics show a direct relationship between a_w and EMC.

3.3 Fitting of sorption model

Table 4 summarizes the results of regression analysis for fitting the EMC data to various models, and the model fitting criteria. All five models produced r^2 close to 1 at all three temperatures. Considering MRE%, RMSE and residual plot requirements, the Peleg model was found to be the most suitable. Except for a RMSE value at 25 ^{o}C, the GAB model satisfied all the selection criteria at all three temperatures. The Oswin model suited all criteria better at 35 ^{o}C. At 25 ^{o}C it indicated a MRE >15% and at 45 ^{o}C there was a residual plot pattern. The Halsey model was more satisfactory at 45 ^{o}C. At 25 ^{o}C it indicated a pattern shape and at 35 ^{o}C the MRE was ≈ 10%. The Henderson model produced a pattern plot at 35 ^{o}C and 45 ^{o}C, and a >10% MRE at all the temperatures. Hence, the Peleg model can be considered as the best fit, followed by the GAB model for EMCs of microwave-convective hot air dried JP within the temperature range of 25-45 ^{o}C. The Peleg model was found to be suitable by de Santana et al. (2015) for freeze dried jamun

Table 3: The mean equilibrium moisture content (EMC) along with standard deviation (SD) of jamun powder (JP) for varying a_w at 25 ^oC, 35 ^oC and 45 ^oC

Salt solutions used for generation of a_w	**a_w**	**25 ^oC EMC (%, db)±SD$^\Psi$**	**a_w**	**35 ^oC EMC (%, db)±SD$^\Psi$**	**a_w**	**45 ^oC EMC (%, db)±SD$^\Psi$**
Lithium chloride (LiCl)	0.114	4.43±0.36	0.113	3.38±0.37$^\#$	0.112	2.82±0.31
Potassium acetate (CH_3COOK)	0.237	6.09±0.27	0.215	4.73±0.64$^\#$	0.197	4.57±0.27
Magnesium chloride ($MgCl_2$)	0.327	9.98±0.41	0.320	7.51±0.44	0.311	6.73±0.11
Potassium carbonate (K_2CO_3)	0.443	12.84±0.24	0.436	10.72±0.94	0.429	10.51±0.27
Magnesium nitrate {$Mg(NO_3)_2$}	0.536	16.52±0.47	0.515	14.25±2.49	0.497	12.07±0.26
Sodium nitrate ($NaNO_3$)	0.742	30.59±0.53	0.720	27.12±1.65	0.699	24.89±0.42
Sodium chloride (NaCl)	0.752	32.20±0.24	0.748	29.64±1.37	0.745	31.16±0.84
Potassium chloride (KCl)	0.855	43.17±0.19	0.822	41.19±0.64	0.791	40.09±0.08
	LSD	**0.62**	**LSD**	**2.19**	**LSD**	**0.68**

Ψ, Average of three replications ± SD; #, indicates no significant difference between the values.

pulp isotherms.

3.4 Moisture sorption isotherms

Figure 2 illustrates the MSIs of JP at 25 ^oC, 35 ^oC and 45 ^oC, as fitted by the Peleg model. Depending on slope, the MSIs can be divided into three zones. At any temperature, the EMC of JP increased relatively slowly at a_ws within $\approx$ 0.1-0.5, compared to the region beyond 0.5 a_w where sharp increases were observed. Thus, shape of the isotherms indicates Type III behaviour, which is a characteristic of foods rich in soluble components (Rizvi, 2014). JP contains about 45% reducing sugars (db) with glucose itself amounting to about 19% (db) (obtained in different experiments not included here). The observed trend of moisture sorption can be attributed to the dissolution tendency of fruit sugars in the absorbed moisture (Maroulis, Tsami, Marinos-Kouris, & Saravacos, 1988). A similar kind of sorption trend was also noticed for sugar-rich foods such as tomato pulp powder (Goula, Karapantsios, Achilias, & Adamopoulos, 2008), grapes, apples (Kaymak-Ertekin & Gedik, 2004) and orange juice powder (Sormoli & Langrish, 2015). Since EMC underwent a sharp increase beyond 0.5 a_w, it can be said that, at RH higher than 50%, JP needs special storage conditions to inhibit several possible degradation reactions. da Silva, Meller da Silva, and Pena (2008) also voiced a similar opinion in their study.

In Figure 2, the EMC decreased with increasing temperature (25 ^oC >35 ^oC >45 ^oC) at any value of a_w up to about 0.75, with slopes being higher than that exhibited below 0.5 a_w. The decrease in the total number of active sites as a consequence of temperature induced physical/chemical changes may result in the fall of EMC (Chowdhury & Das, 2012; Muzaffar & Kumar, 2016). At increased temperatures, water molecules because of their activation at higher energy levels gain higher mobility, become unstable and break away from the binding sites, thereby causing a reduction in EMC, as explained by Menkov and Durakova (2007). According to de Santana et al. (2015) and Al-Muhtaseb et al. (2002), the water vapour pressure (WVP) on powder surfaces increases at higher temperatures, allowing the water molecules to get detached from the binding sites. Interestingly for a_w higher than 0.75, the increase in EMC with a_w is even higher than for the previously displayed regions. Moreover, a crossover is seen so that the EMCs follow the order: 45 ^oC >35 ^oC >25 ^oC. As described by Basu, Shivhare, and Muley (2013) and Labuza and Altunakar (2007), such crossover at high water activity is mainly due to increased solubility of sugar and dissolution of new solutes at higher temperatures. Also, at high water activity the soluble components absorb more water, which is further accentuated by the temperature (Basu et al., 2013).

Table 4: Model coefficients and error terms for different sorption models

Temp (°C)	EMC Model	A	B	C	D	r^2	RMSE	MRE (%)	Residual Plot
	Peleg	**30.3963**	**0.9989**	**36.8762**	**5.0221**	**0.9946**	**0.8827**	**7.8715**	**Random**
	GAB	11.1246	5.2765	0.8781	-	0.9874	1.4263	9.1236	Random
25	Oswin	16.4801	0.5272	-	-	0.9844	1.8427	15.4206	Random
	Henderson	0.0198	1.2322	-	-	0.9960	1.8681	12.4555	Random
	Halsey	38.0501	1.4649	-	-	0.9740	2.4035	19.5301	Pattern
	Peleg	**23.9963**	**0.9999**	**67.8792**	**5.9221**	**0.9875**	**0.4133**	**5.1785**	**Random**
	GAB	9.5502	2.9603	0.9584	-	0.9848	0.3629	4.8470	Random
35	Oswin	13.4154	0.7336	-	-	0.9858	0.3076	4.0173	Random
	Henderson	0.0740	0.8542	-	-	0.9956	0.9373	10.6109	Pattern
	Halsey	10.4390	1.0626	-	-	0.9765	0.8959	9.9953	Random
	Peleg	**23.0082**	**0.9978**	**123.3597**	**7.3802**	**0.9802**	**0.2312**	**2.5248**	**Random**
	GAB	7.3339	3.9545	1.0452	-	0.9798	0.2416	2.0775	Random
45	Oswin	12.7807	0.8417	-	-	0.9905	0.6595	6.8383	Pattern
	Henderson	0.0478	1.0028	-	-	0.9984	3.0425	10.5552	Pattern
	Halsey	6.6982	0.9085	-	-	0.9837	0.3622	4.4701	Random

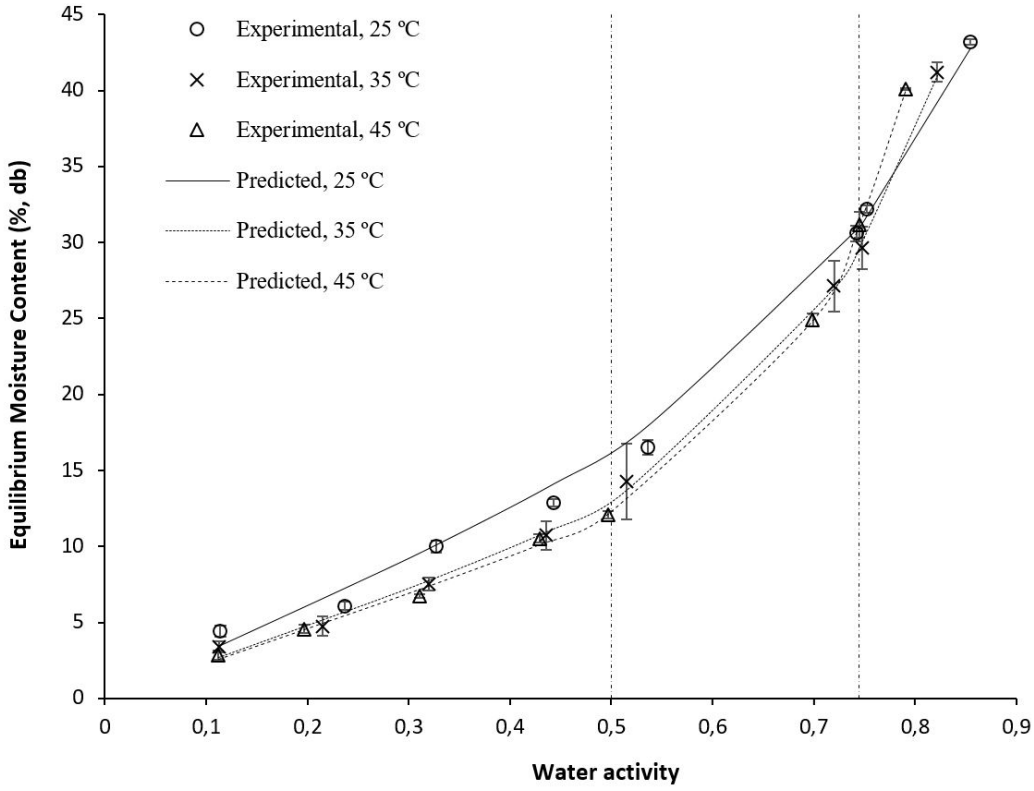

Figure 2: Effect of temperature on moisture sorption isotherm of JP as expressed by the Peleg model

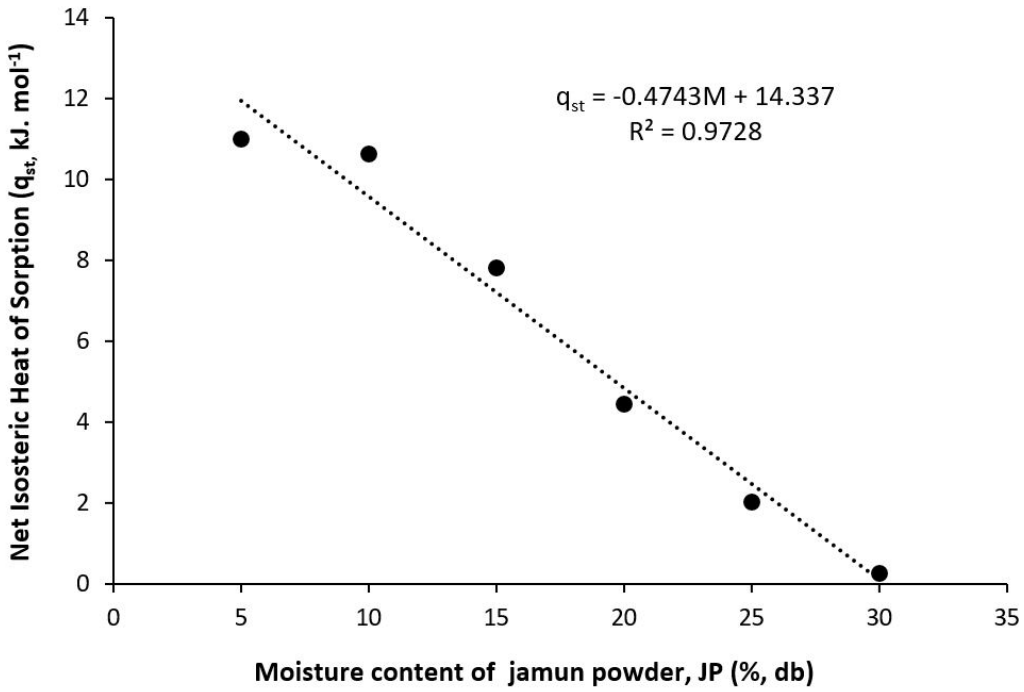

Figure 3: Variation in net isosteric heat of sorption (q_{st}) of jamun powder (JP) as a function of moisture content

3.5 Net isosteric heat of sorption (q_{st})

The absolute value of q_{st} (Eq. 4) of JP as a function of moisture content is represented in Figure 3. Mathematically, the trend is represented by the following linear relation (Eq. 10), and the resulting r^2 justifies the appropriateness of the fit.

$$q_{st} = -0.4743M + 14.337; r^2 = 0.9728 \quad (10)$$

where M is the moisture content in %, db. Thus, the q_{st} decreases with the increase in moisture content from 11.02 kJ. mol^{-1} at 5% moisture to 0.27 kJ.mol^{-1} at 30%, thus approaching the heat of vaporization of pure water. The linear decreasing trend of q_{st} was also observed by de Santana et al. (2015) for freeze dried jamun pulp and by Basu et al. (2013) for pectin. It may be worth mentioning that the maximum q_{st} in this study is comparable with the value for orange juice powder (9.05 kJ. mol^{-1}) calculated by Sormoli and Langrish (2015).

Since higher the value of q_{st} means higher is the degree of binding, the water molecules become tightly bound to the active sites on the surface of the JP at low moisture contents (Sormoli & Langrish, 2015). As explained by Iglesias and Chirife (1982), sorption occurs initially at the most active sites involving higher interaction energy. As active sites get exhausted, moisture binding starts at less active sites producing less heat of sorption.

3.6 Spreading pressure (Φ)

The value of Φ increases, almost linearly, with increase of a_w (Figure 4). At any a_w, Φ decreases for an increase of temperature from 25 ^{o}C to 35 ^{o}C. However, for further increase to

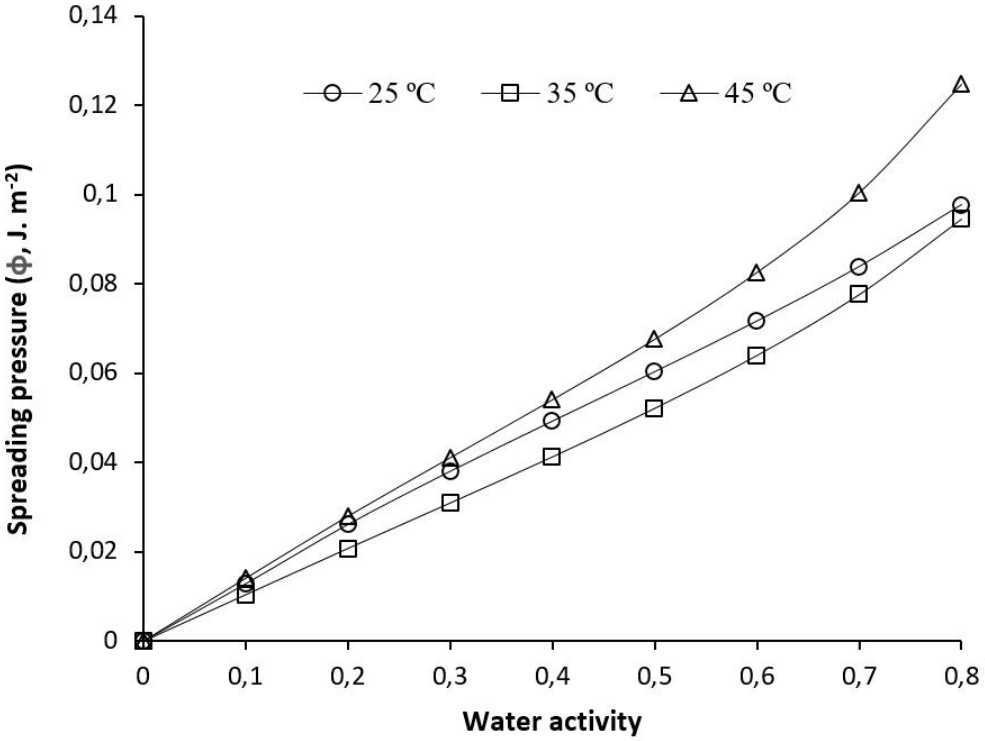

Figure 4: Variation in spreading pressure (Φ) with water activity (a_w) at 25 ^{o}C, 35 ^{o}C and 45 ^{o}C

45 ^{o}C, Φ increased to levels even higher than that at 25 ^{o}C and the differences in Φ further increased for a_w from 0.3 onwards. It may be stated that the effect of temperature on Φ is case specific, depending on composition of the sorbent. Depending on temperature, Φ may be increasing/decreasing/decreasing then increasing/increasing then decreasing (Aviara & Ajibola, 2002; Lago et al., 2013; Al-Muhtaseb et al., 2004; Togrul & Arslan, 2007). Similar observations, as for the present study, were reported for high amylose starch powder (Al-Muhtaseb et al., 2004) at 30-60 ^{o}C, and walnut kernel (Togrul & Arslan, 2007) at 25-45 ^{o}C.

Spreading pressure is the driving force for diffusion of moisture in a porous solid (Skaar & Babiak, 1982). Torres, Moreira, Chenlo, and Vazquez (2012) explained that high spreading pressure values indicate a high affinity of water molecules for binding sites. This may lead to swelling in a high RH environment (discussed in section 3.7).

3.7 Net integral enthalpy (Q_{in})

Net integral enthalpy (Q_{in}) of bound water molecules initially decreases up to about 6% moisture content, and then increases for higher moisture content (Figure 5). The decreasing portion probably arises from the monolayer covering of JP (Fasina et al., 1999). At low moisture contents, water is preferentially adsorbed on the most accessible locations on the exterior surface of the solid. Following this, as less favourable sites are filled up, the Q_{in} then gradually declines till there is formation of multi layers of water (Al-Muhtaseb et al., 2004). With still higher moisture content gained in a higher RH atmo-

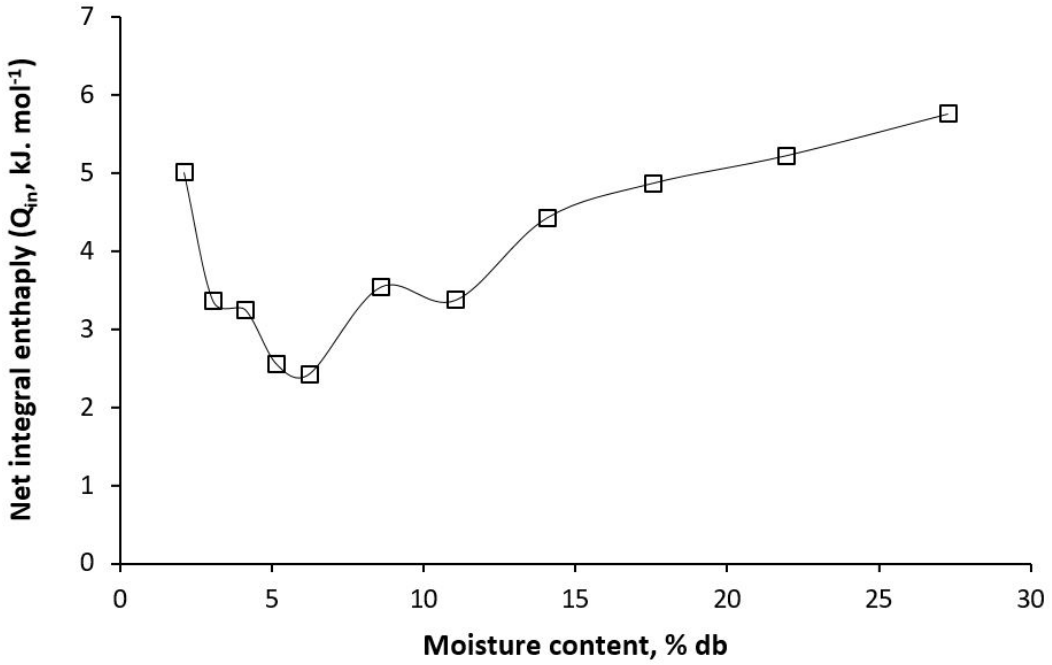

Figure 5: Variation in net integral enthalpy (Q_{in}) of jamun powder (JP) with moisture content

sphere, there is probably swelling of the powder with concomitant exposition of higher and higher energy binding sites that require increasingly higher Q_{in} involvement. Such a decreasing, followed by increasing, profile has been documented for mango skin (Ferreira de Souza et al., 2015) and orange peel (Villa-Velez, Ferreira de Souza, Ramos, Polachini, & Telis-Romero, 2015). An increase in Q_{in} with increasing moisture content was also reported in studies on cassava (Aviara & Ajibola, 2002) and potato and sweet potato flakes (Lago et al., 2013). In the case of walnuts kernels, the Q_{in} increased slightly with increasing moisture content and then remained constant (Togrul & Arslan, 2007).

3.8 Net integral enthalpy (S_{in})

Net integral entropy (S_{in}) of the adsorbed water molecules was found to decrease continually with moisture content of JP (Figure 6). The loss in entropy, in general, indicates the loss of rotational freedom or randomness of the adsorbate molecules. On exposure to low RH/a_w, the easily available sites on the surface become filled, where in addition to ligand–substrate binding, lateral interactions in the adsorbed molecules also contribute to reduction in randomness (Aviara & Ajibola, 2002). At increasingly higher RH, there is attainment of a higher EMC leading to structural transformation arising from solubilisation of ingredients and swelling of the powder which ultimately opens more and more sites to bind water molecules (McMinn & Magee, 2003; Zhang, Bai, Zhao, & Duan, 2016). In Figure 6, the maximum values of S_{in} were found at the moisture content of around 1% (db) and can be considered as the zone of most energetic water molecules in the material. Following this, up to about 8% db moisture content, S_{in} decreased but remained in a positive zone. With >8% moisture, the values were all negative. Similar profiles of S_{in}, covering both positive and negative zones, have been reported for moisture sorption of mango skin (Fer-

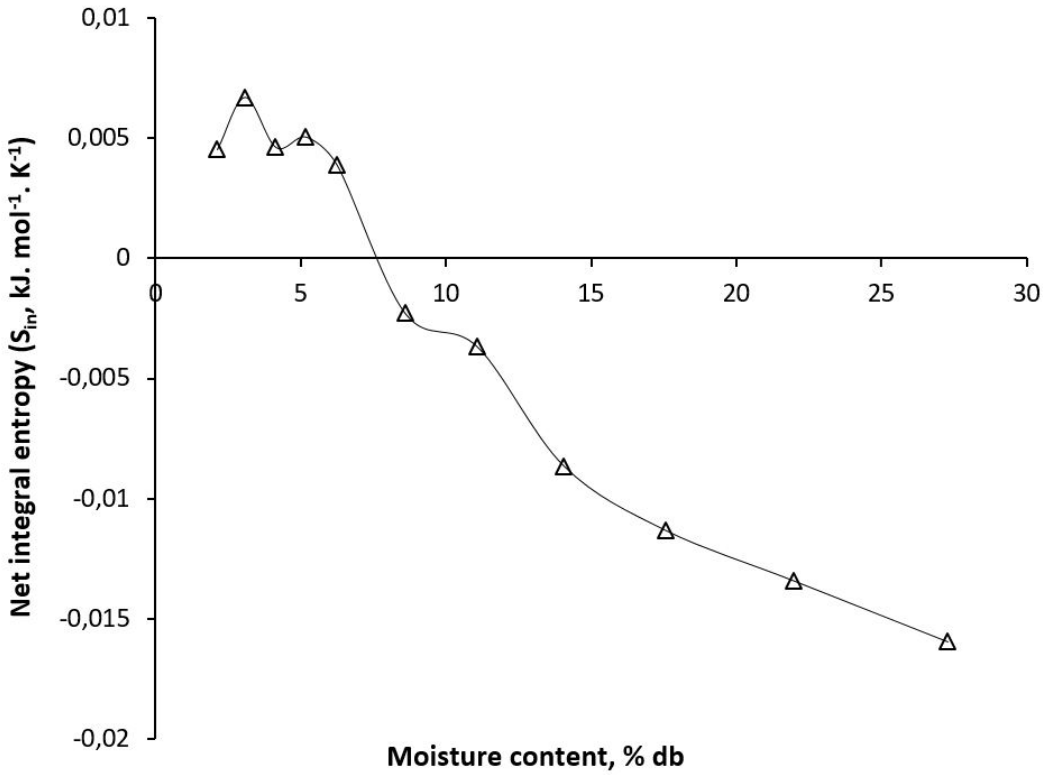

Figure 6: Variation in net integral entropy (S_{in}) of jamun powder (JP) with moisture content

reira de Souza et al., 2015) and gari (Aviara & Ajibola, 2002). For mango skin adsorption, the negative value was also comparable to JP. Iglesias, Chirife, and Viollaz (1976) explained that negative values of S_{in} might be attributed to the existence of chemical adsorption and/or structural modifications of the adsorbent, while Rizvi (2014) attributed it to the fact that the products contain more polar groups, which bind water more strongly.

The minimum integral entropy zone corresponds to maximum stability of food products, since in this zone the water molecules are well accommodated and less available to take part in deteriorating reactions. In the case of JP where S_{in} is gradually decreasing, probably due to structural modification (as mentioned above), the minimum integral entropy zone can be considered corresponding to the monolayer moisture content (Ferreira de Souza et al., 2015). Thus from Table 4, the safe moisture content may be in the zone of 7-11% (GAB monolayer value) for the temperature range of 45–25 ^{o}C.

4 Conclusions

Jamun seed kernel powder could be added to jamun pulp powder at a level of 2% (db) without affecting the sensorial acceptance of the pulp powder in the mixture, finally named as jamun powder (JP). The EMC of JP decreased with increasing temperature (25 ^{o}C >35 ^{o}C >45 ^{o}C) at any constant value of a_w up to about 0.75, and the Peleg model could satisfactorily describe the moisture sorption isotherms within 25-45 ^{o}C. Over the range of EMC from 5-30%, the q_{st} decreased linearly from 11.02 kJ. mol^{-1} to 0.27 kJ. mol^{-1}. The Φ increased with increasing a_w, and

with respect to temperature it followed the order: 45 ^{o}C >25 ^{o}C >35 ^{o}C. Net integral enthalpy (Q_{in}) displayed a decreasing trend till 6% moisture content of JP, followed by an increasing pattern thereafter for higher moisture contents. Net integral entropy (S_{in}) was observed to decrease continuously with the increase in moisture content, and the monolayer moisture content 7-11% may be regarded as the safe moisture content zone for JP within the temperature range of 45-25 ^{o}C.

References

Arslan, N., & Togrul, H. (2005). Modelling of water sorption isotherms of macaroni stored in a chamber under controlled humidity and thermodynamic approach. *Journal of Food Engineering*, *69*(2), 133–145. doi:10.1016/j.jfoodeng.2004.08.004

Aviara, N. A., & Ajibola, O. O. (2002). Thermodynamics of moisture sorption in melon seed and cassava. *Journal of Food Engineering*, *55*(2), 107–113. doi:10.1016/S0260-8774(02)00023-7

Basu, S., Shivhare, U. S., & Muley, S. (2013). Moisture adsorption isotherms and glass transition temperature of pectin. *Journal of Food Science and Technology-mysore*, *50*(3), 585–589. doi:10.1007/s13197-011-0327-y

Bhattacharya, M., Srivastav, P. P., & Mishra, H. N. (2015). Thin-layer modeling of convective and microwave-convective drying of oyster mushroom (*Pleurotus ostreatus*). *Journal of Food Science and Technology-mysore*, *52*(4), 2013–2022. doi:10.1007/s13197-013-1209-2

Biswal, S., Mohapatra, M., Panda, M. K., & Dash, S. K. (2017). Moisture desorption isotherms of fresh jamun (*Syzygium cumini*) fruit. *Indian Journal of Agricultural Research*, *51*(3), 267–271.

Chowdhury, T., & Das, M. (2010). Moisture sorption isotherm and isosteric heat of sorption characteristics of starch based edible films containing antimicrobial preservative. *International Food Research Journal*, *17*(3), 601–614. Retrieved from http://www.ifrj.upm.edu.my/17%5C%20(03)%5C%202010/IFRJ-2010-601-614%5C%20India.pdf

Chowdhury, T., & Das, M. (2012). Moisture sorption isotherm and isosteric heat of sorption of edible films made from blends of starch, amylose and methyl cellulose. *International Food Research Journal*, *19*(4), 1669–1678. Retrieved from http://www.ifrj.upm.edu.my

da Silva, A. E., Meller da Silva, L. H., & Pena, R. d. S. (2008). Hygroscopic behavior of acai and cupuacu powders. *Ciencia E Tecnologia De Alimentos*, *28*(4), 895–901. doi:10.1590/S0101-20612008000400020

Das, I., & Arora, A. (2018). Alternate microwave and convective hot air application for rapid mushroom drying. *Journal of Food Engineering*, *223*, 208–219. doi:10.1016/j.jfoodeng.2017.10.018

de Santana, R. F., de Oliveira Neto, E. R., Santos, A. V., Faria Soares, C. M., Lima, A. S., & Cardoso, J. C. (2015). Water sorption isotherm and glass transition temperature of freeze-dried *Syzygium cumini* fruit (jambolan). *Journal of Thermal Analysis and Calorimetry*, *120*(1), 519–524. doi:10.1007/s10973-014-4014-x

Dey Paul, I., & Das, M. (2017). Effect of maltodextrin, tricalcium phosphate and glycerol monostearate on moisture sorption characteristics of jamun (*Syzygium cumini L.*) pulp powder. In Proceedings of *International Food Research Conference*, held at Universiti Putra Malaysia, Malaysia. (p. 87). 25-27 July.

Fasina, O. O., Ajibola, O. O., & Tyler, R. T. (1999). Thermodynamics of moisture sorption in winged bean seed and gari. *Journal of Food Process Engineering*, *22*(6), 405–418. doi:10.1111/j.1745-4530.1999.tb00496.x

Ferrari, C. C., Marconi Germer, S. P., Alvim, I. D., Vissotto, F. Z., & de Aguirre, J. M. (2012). Influence of carrier agents on the physicochemical properties of blackberry powder produced by spray drying. *International Journal of Food Science and Technology*, *47*(6), 1237–1245. doi:10.1111/j.1365-2621.2012.02964.x

Ferreira de Souza, S. J., Alves, A. I., Rufino Vieira, E. N., Gomez Vieira, J. A., Ramos, A. M., & Telis-Romero, J. (2015). Study of thermodynamic water properties and moisture sorption hysteresis of mango skin. *Food Science and Technology*, *35*(1), 157–166. doi:10.1590/1678-457X.6557

Goula, A. M., Karapantsios, T. D., Achilias, D. S., & Adamopoulos, K. G. (2008). Water sorption isotherms and glass transition temperature of spray dried tomato pulp. *Journal of Food Engineering*, *85*(1), 73–83. doi:10.1016/j.jfoodeng.2007.07.015

Horuz, E., Bozkurt, H., Karatas, H., & Maskan, M. (2017). Drying kinetics of apricot halves in a microwave-hot air hybrid oven. *Heat and Mass Transfer*, *53*(6), 2117–2127. doi:10.1007/s00231-017-1973-z

Ibanoglu, S., Kaya, S., & Kaya, A. (1999). Evaluation of sorption properties of Turkish tarhana powder. *Food / Nahrung*, *43*(2), 122–125. doi:10.1002/(SICI)1521-3803(19990301)43:2⟨122::AID-FOOD122⟩3.0.CO;2-3

Igathinathane, C., Womac, A. R., Sokhansanj, S., & Pordesimo, L. O. (2007). Moisture sorption thermodynamic properties of corn stover fractions. *Transactions of the Asabe*, *50*(6), 2151–2160. Annual Meeting of the American-Society-of-Agricultural-and-Biological-Engineers, Univ Wisconsin-Madison, Madison, WI, NOV 09-12, 2005.

Iglesias, H. A., & Chirife, J. (1982). Handbook of food isotherms: Water sorption parameters for food and food components. (Chap. Mathematical description of isotherms, pp. 262–335). New York: Academic Press.

Iglesias, H. A., Chirife, J., & Viollaz, P. (1976). Thermodynamics of water vapour sorption by sugar beet root. *International Journal of Food Science & Technology*, *11*(1), 91–101. doi:10.1111/j.1365-2621.1976.tb00705.x. eprint: https://onlinelibrary.wiley.com/doi/pdf/10.1111/j.1365-2621.1976.tb00705.x

Kamal, A. (2014). Phytochemical screening of *Syzygium cumini* seeds. *Indian Journal of Plant Sciences*, *3*(4), 1–4.

Kapoor, A., & Iqbal, H. (2013). Efficiency of tannase produced by Trichoderma harzianum MTCC 10841 in pomegranate juice clarification and natural tannin degradation. *International Journal of Biotechnology and Bioengineering Research*, *4*(6), 641–650.

Kaymak-Ertekin, F., & Gedik, A. (2004). Sorption isotherms and isosteric heat of sorption for grapes, apricots, apples and potatoes. *LWT - Food Science and Technology*, *37*(4), 429–438. doi:10.1016/j.lwt.2003.10.012

Kumar, D., Prasad, S., & Murthy, G. S. (2014). Optimization of microwave-assisted hot air drying conditions of okra using response surface methodology. *Journal of Food Science and Technology-mysore*, *51*(2), 221–232. doi:10.1007/s13197-011-0487-9

Labuza, T. P., & Altunakar, B. (2007). Water activity in foods: Fundamentals and applications. In G. V. Barbosa-Canovas, J. A. J. Fontana, S. J. Schmidt, & T. P. Labuza (Eds.), (Chap. Water activity prediction and moisture sorption isotherms, pp. 109–154). Blackwell Publishing, Oxford, UK.

Lago, C. C., Liendo-Cardenas, M., & Zapata Norena, C. P. (2013). Thermodynamic sorption properties of potato and sweet potato flakes. *Food and Bioproducts Processing*, *91*(C4), 389–395. doi:10.1016/j.fbp.2013.02.005

Lomauro, C. J., Bakshi, A. S., & Chen, J. Y. (1985). Evaluation of food moisture sorption isotherm equations. Part I: Fruit, vegetable and meat products. *LWT - Food Science and Technology*, *18*, 111–117.

Maroulis, Z. B., Tsami, E., Marinos-Kouris, D., & Saravacos, G. D. (1988). Application of the GAB model to the moisture sorption isotherms for dried fruits. *Journal of Food Engineering*, *7*(1), 63–78. doi:10.1016/0260-8774(88)90069-6

McMinn, W. A. M., & Magee, T. R. A. (2003). Thermodynamic properties of moisture sorption of potato. *Journal of Food Engineering*, *60*(2), 157–165. doi:10.1016/S0260-8774(03)00036-0

Menkov, N. D., & Durakova, A. G. (2007). Moisture sorption isotherms of sesame flour at

several temperatures. *Food Technology and Biotechnology*, *45*(1), 96–100.

Monica, N., Dey Paul, I., & Das, M. (2016). Microwave-convective hot air and vacuum drying of jamun seed powder. In H. N. Mishra, S. L. Srivastava, P. P. Srivastava, & P. P. Tripathy (Eds.), *Food process engineering and technology* (Vol. Papers presented at International Conference on Emerging Technologies in Agricultural and Food Engineering, held at Indian Institute of Technology Kharagpur, India, 27-30 December, pp. 311–323). New Delhi: Excel India Publishers.

Al-Muhtaseb, A. H., McMinn, W. A. M., & Magee, T. R. A. (2002). Moisture sorption isotherm characteristics of food products: A review. *Food and Bioproducts Processing*, *80*(2), 118–128. doi:10 . 1205 / 09603080252938753

Al-Muhtaseb, A. H., McMinn, W. A. M., & Magee, T. R. A. (2004). Water sorption isotherms of starch powders. part 2: Thermodynamic characteristics. *Journal of Food Engineering*, *62*(2), 135–142. doi:10.1016/S0260-8774(03)00202-4

Muzaffar, K., & Kumar, P. (2016). Moisture sorption isotherms and storage study of spray dried tamarind pulp powder. *Powder Technology*, *291*, 322–327. doi:10.1016/j.powtec.2015.12.046

Paul, I. D., & Das, M. (2018). Effect of freeze, microwave-convective hot air, vacuum and dehumidified air drying on total phenolics content, anthocyanin content and antioxidant activity of jamun (*Syzygium cumini L.*) pulp. *Journal of Food Science and Technology-mysore*, *55*(7), 2410–2419. doi:10.1007/s13197-018-3158-2

Ranganna, S. (1986). Handbook of analysis and quality control for fruit and vegetable products. (Chap. Sensory Evaluation, pp. 594–645). Tata McGraw-Hill Education.

Rizvi, S. S. H. (2014). Thermodynamic properties of foods in dehydration. In *Engineering properties of foods, third edition* (pp. 359–435). CRC Press.

Schiffmann, R. F. (1992). Microwave processing in the US food industry. *Food Technology*.

Sehwag, S., & Das, M. (2015). Nutritive, therapeutic and processing aspects of jamun, *Syzygium cuminii (L.)* skeels-an overview. *Natural Product Radiance*, *5*, 295–307.

Sehwag, S., & Das, M. (2016). Composition and antioxidant potential of jamun (*Syzygium cumini L.*) from eastern india. *Asian Journal of Biochemical and Pharmaceutical Research*, *6*, 106–121.

Sharma, G. P., & Prasad, S. (2001). Drying of garlic (allium sativum) cloves by microwave-hot air combination. *Journal of Food Engineering*, *50*(2), 99–105. doi:10.1016/S0260-8774(00)00200-4

Skaar, C., & Babiak, M. (1982). A model for bound-water transport in wood. *Wood Science and Technology*, *16*(2), 123–138. doi:10.1007/BF00351098

Sormoli, M. E., & Langrish, T. A. G. (2015). Moisture sorption isotherms and net isosteric heat of sorption for spray-dried pure orange juice powder. *LWT - Food Science and Technology*, *62*(1, 2, SI), 875–882. doi:10.1016/j.lwt.2014.09.064

Togrul, H., & Arslan, N. (2007). Moisture sorption isotherms and thermodynamic properties of walnut kernels. *Journal of Stored Products Research*, *43*(3), 252–264. doi:10.1016/j.jspr.2006.06.006

Torres, M. D., Moreira, R., Chenlo, F., & Vazquez, M. J. (2012). Water adsorption isotherms of carboxymethyl cellulose, guar, locust bean, tragacanth and xanthan gums. *Carbohydrate Polymers*, *89*(2), 592–598. doi:10.1016/j.carbpol.2012.03.055

Villa-Velez, H. A., Ferreira de Souza, S. J., Ramos, A. P., Polachini, T., & Telis-Romero, J. (2015). Thermodynamic properties of water adsorption from orange peels. *Journal of Bioenergy and Food Science*, *2*(2), 72–81. doi:10.18607/jbfs.v2i2.32

Zhang, H., Bai, Y., Zhao, X., & Duan, R. (2016). Water desorption isotherm and its thermodynamic analysis of glutinous rice flour. *American Journal of Food Technology*, *11*(4), 115–124. Retrieved from 10 . 3923/ajft.2016.115.124